2021 43rd Annual International Conference of the
IEEE Engineering in Medicine & Biology Society (EMBC)
Oct 31 - Nov 4, 2021. Virtual Conference

Design of Bionic Prosthetic Fingers Using 3D Topology Optimization

Yilun Sun, *Graduate Student Member, IEEE*, and Tim C. Lueth, *Senior Member, IEEE*

***Abstract*— Compliant mechanisms are frequently used in the design of prosthetic fingers since their monolithic structure and flexible movement are quite similar to the biological human fingers. However, the design of compliant prosthetic fingers is not easy, as the conventional rigid-link-based mechanism theory cannot be directly applied. In this paper, we introduce a 3D topology optimization based design framework to simplify the synthesis process of bionic compliant prosthetic fingers. The proposed framework is implemented in the software MATLAB and the realized fingers can be quickly fabricated using selective laser sintering (SLS) technology. To illustrate the design process of the proposed framework, a design example was presented. The bending performance of the realized finger was successfully verified by the FEM-based simulation and the payload test. In future work, the optimized fingers have the potential to be integrated into prosthetic hands to realize sophisticated grasping movements.**

I. Introduction

Amputations in the hand are usually the result of a traumatic accident or a planned operation that prevents the spread of diseases in an infected finger or hand. In order to rebuild the physical abilities of the patients' hands, various prosthetic hands and fingers were developed [1]. From the mechanism design point of view, the conventional prosthetic fingers use the rigid-link-based mechanism to realize the finger movement. A typical example of that is the DLR Hand II [2], which is a dexterous and robust anthropomorphic hand arm system with electrical actuation. To achieve high mechanical performance, another rigid-link-based prosthetic hand, the Delft Cylinder Hand [3], uses hydraulic actuation and is designed with light weight. Other research studies also tried to fabricate prosthetic fingers using additive manufacturing technologies. For example, authors in [4] used 3D scanner to copy the shape of a cosmetic prosthetic hand. The measured 3D shape data was then processed and incorporated into the design of a linear-motor-actuated prosthetic hand, which was fabricated using a Fused Deposition Modeling (FDM) printer. Another 3D-printed prosthetic hand, the OLYMPIC [5], was developed with a modular design, in which the fingers with patient-specific size could be easily 3D-printed and attached to the main module.

Although the rigid-link-based mechanisms are generally robust and stable for designing prosthetic fingers, their limitations should also be considered [6]. For example, the assembly process of a high-precision prosthetic hand is very complicated and periodic lubrication is also required for maintenance reasons. To cope with these problems, compliant mechanisms are incorporated into the design of prosthetic hands and fingers, whose motions are derived from the elastic deformation of the flexible parts. In [7], a tendon-driven compliant thumb was developed and integrated into a prosthetic hand, mimicking the grasping and manipulation behavior of a natural hand. Another compliant prosthetic hand was proposed in [8], where the five fingers were all based on cable-driven continuum structures to realize flexible manipulation. However, due to the continuum-structure effect of the compliant mechanisms, it is difficult to model and synthesize compliant prosthetic fingers using the conventional rigid-link-based mechanism theory. To improve the design efficiency, some topology optimization based methods were proposed by researchers to synthesize compliant prosthetic fingers. In [9], the authors designed a discrete-structure-based compliant finger using a 2D topology optimization method. A few studies, such as [10], tried to use 3D topology optimization algorithms to realize pneumatically actuated prosthetic fingers.

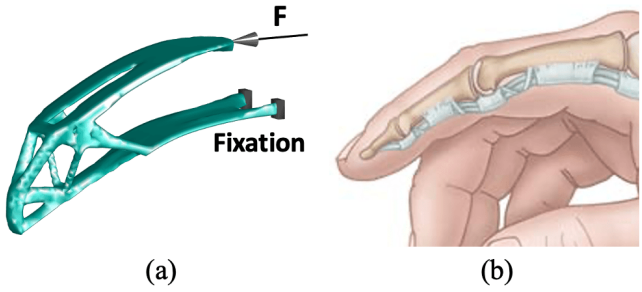

Fig. 1. Comparison of a realized prosthetic finger and a human finger: a) A 3D topology optimized compliant finger, where F indicates the actuation force, b) The biological tendon-driven mechanism of a human finger.

In this paper, we introduce a novel design framework for designing 3D topology optimized compliant prosthetic fingers. Since the topology optimization method is inspired from the biological evolution process, the realized fingers also have bionic shape and flexible bending performance (see Fig. 1). The proposed design framework is implemented in a single developing environment (MATLAB) to improve the efficiency of the code [11]. In combination with the 3D printing technologies, the framework can greatly improve the design efficiency and performance of the prosthetic fingers.

The remainder of the paper is organized as follows: Section II describes the workflow of the design framework and illustrates the mathematical principle of the 3D topology optimization method. A design example is presented in

This work was supported by the Munich School of Robotics and Machine Intelligence (MSRM), Technical University of Munich, Munich, Germany.

The authors are with the Institute of Micro Technology and Medical Device Technology, Technical University of Munich, Munich, Germany (e-mail: yilun.sun@tum.de; tim.lueth@tum.de).

Corresponding author: Yilun Sun.

Algorithm 1: Workflow of the 3D Topology Optimization Based Design Framework

```
Initialization of a cuboid design domain with the size of {n_x,n_y,n_z};
Define the corresponding boundary conditions and the objective function f(x) of the design problem;
while Convergence criteria are not fulfilled do
    Finite element analysis;
    Calculate the objective function f;
    Update of the density distribution x according to the result of sensitivity analysis;
Post-processing of x to get a 3D-printable surface model for prototyping the prosthetic finger;
```

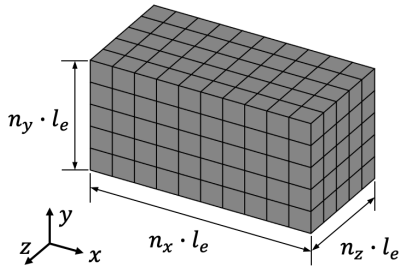

Fig. 2. A cuboid design domain that is meshed into $n_x \times n_y \times n_z$ cubic elements. The side length of each cubic element id l_e.

Section III to demonstrate the performance of the framework. Section IV concludes the entire paper and outlines the future work.

II. Methodology

A. Design Workflow

Algorithm 1 presents the generalized workflow of the proposed design framework. Firstly, the user creates a 3D design domain for the prosthetic finger, which is a cuboid meshed into $n_x \times n_y \times n_z$ cubic elements (see Fig. 2). Then, the boundary conditions of the design problem, such as the actuation forces and the bending directions, should be defined to describe the design objective $f(\mathbf{x})$ of the expected prosthetic finger. After that, the shape synthesis process begins by performing the 3D topology optimization. During the optimization process, 3D finite element analysis (FEA) is performed in each step to calculate the predefined objective function. The distribution $\mathbf{x}$ of the normalized material density in the design domain is then iteratively modified according to an updating scheme. After the optimization process converges, post-processing techniques are performed to obtain a 3D-printable and functional prosthetic finger.

B. Algorithm of the 3D Topology Optimization Method

The objective of the proposed 3D topology optimization method is to search for an almost solid-void (1-0) normalized density distribution $\mathbf{x}$ (a voxel model) in the 3D design domain to achieve the maximum displacement of a certain output point $\boldsymbol{P}_{out}$. The voxel model $\mathbf{x}$ is implemented as a MATLAB array whose size is (n_x,n_y,n_z). The objective function can be formulated as:

$$\left.\begin{aligned} \max_{\mathbf{x}}: \quad & f(\mathbf{x}) = \mathbf{L^T U} = u_{out} \\ \text{subject to}: \quad & \sum_{e=1}^{N} v_e x_e \le V_0 c \\ : \quad & \mathbf{KU} = \mathbf{F}\ ,\ \mathbf{K} = \sum_{e=1}^{N} \mathbf{K_e}(E_e) \\ : \quad & E_e = E_0 x_e^p\ ,\ 0 < x_e \le 1 \end{aligned}\right\} \tag{1}$$

where $\mathbf{U}$ is the displacement vector of all nodes in the design domain and $\mathbf{L}$ is a vector used to select the output displacement u_{out} from $\mathbf{U}$. c is a volume fraction factor that constrains the volume of the realized finger. 3D FEA is used to calculate $\mathbf{U}$, where $\mathbf{K}$ and $\mathbf{F}$ are the global stiffness matrix and the global load vector respectively. Since $\mathbf{x}$ is not directly correlated to the stiffness matrix $\mathbf{K}$, we use $E_e = E_0 x_e^p$ to involve $\mathbf{x}$ into the FEA, where E_0 is the elastic modulus of the full-density material. p is a penalty number.

To solve the optimization problem, $\mathbf{x}$ is updated iteratively. The corresponding update algorithm can be illustrated as in Algorithm 2. In the presented algorithm, m is a predefined move limit of x_e in each step, while η is a damping factor. These two parameters are introduced to maintain the numerical stability of $\mathbf{x}$.

Algorithm 2: The Iterative Update Algorithm of $\mathbf{x}$

```
Perform the sensitivity analysis B_e ← −∂u_out/∂x_e / (λ_1 v_e);
x_e^- ← max(x_min, x_e − m);
x_e^+ ← min(1, x_e + m);
if x_e B_e^η ≤ x_e^- then
    x_e,updated ← x_e^-;
else if x_e^- < x_e B_e^η < x_e^+ then
    x_e,updated ← x_e B_e^η;
else
    x_e,updated ← x_e^+;
```

An almost solid-void (1-0) distribution of $\mathbf{x}$ is reached when the convergence criteria are fulfilled. In the post-processing, to create a surface model of the realized prosthetic finger, the marching cubes algorithm [12] is used to extract an iso-surface from $\mathbf{x}$. Finally, the calculated finger model can be 3D-printed for prototyping and testing.

III. Design Example

In this section, the design and test of a bionic compliant prosthetic finger is presented to demonstrate the performance of the proposed design framework.

A. Synthesis and Fabrication of a Prosthetic Finger

Fig. 3 is a schematic diagram showing the design problem of the compliant finger. It can be seen that, the design domain is a blue cuboid comprised of $80 \times 20 \times 10$ cubic elements with $l_e = 0.5mm$. Since the prosthetic finger is

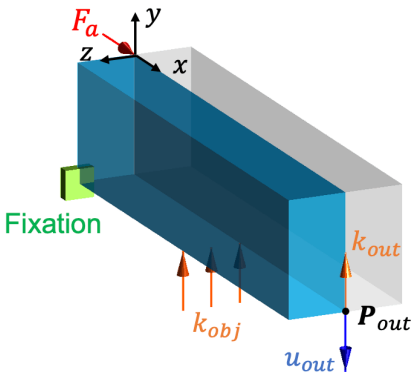

Fig. 3. Schematic diagram illustrating the design problem of the prosthetic finger.

supposed to have a symmetric structure, we defined the right surface of the design domain (the x-y plane in Fig. 3) as the symmetric surface and all the boundary conditions were also mirrored. In this way, the predefined design domain was used to synthesize only half of the finger, which reduced the computational cost greatly. A displacement-based push force F_a of $5\,\mathrm{mm}$ was applied on the design domain to actuate the compliant finger, while the blue arrow indicated the output displacement u_{out}. $k_{obj} = 0.75N/mm$ and $k_{out} = 0.5N/mm$ were linear springs applied on the middle and end of the finger in x-axis, in order to imitate the grasping resistance on the finger joint and tip, respectively. The green domain depicted the fixation boundary condition. Since the compliant finger was SLS-printed with the polyamide (PA2200), which is a linearly elastic material, the Young's modulus E_0 and Poisson's ratio ν were set to $1700\,\mathrm{MPa}$ and 0.3 according to its data sheet.

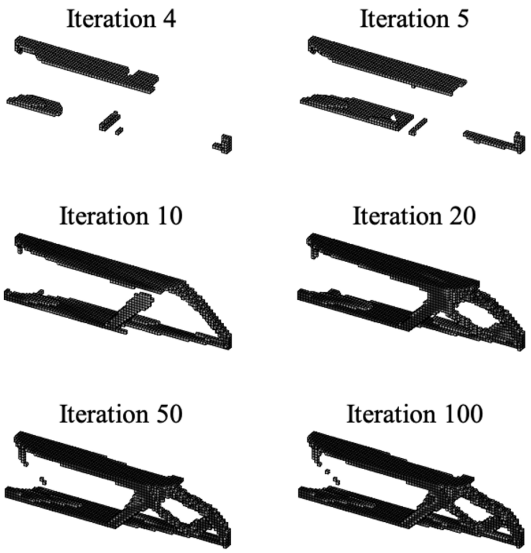

Fig. 4. The evolution of $\mathbf{x}$ during the 3D topology optimization process, where $f(\mathbf{x})$ converged at the 100^{th} iteration. The elements with $x_e > 0.5$ are plotted and the black color represents solid element in the design domain.

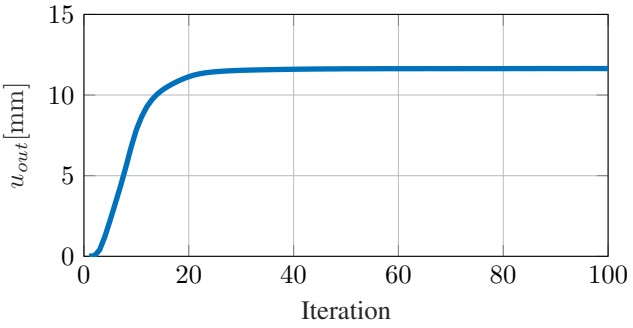

Fig. 5. The value of $f(\mathbf{x})$ in the optimization process.

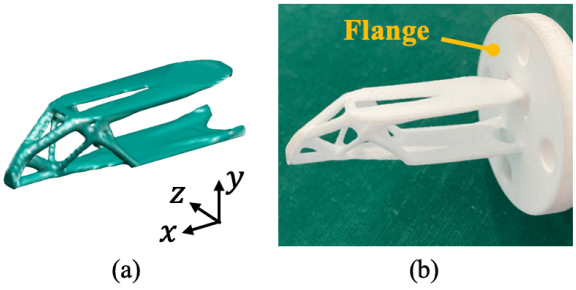

Fig. 6. The realized prosthetic finger: a) The surface model, b) The SLS-printed prototype.

Fig. 4 shows the evolution process of $\mathbf{x}$ to achieve the final topology, where the objective function converged at the 100^{th} iteration. The maximum u_{out} has reached $11.64\,\mathrm{mm}$, as is shown in the diagram in Fig. 5. After post-processing, a symmetrical and monolithic bionic finger was realized (see Fig. 6a), which was then SLS-printed for testing the bending performance. In the prototype, a flange was also constructed (see Fig. 6b) so that the finger could be fixed and then actuated by servo motor.

B. FEM-Based Simulation

Large-displacement FEA [6] was conducted to analyze the stress distribution of the realized bionic finger during the bending movement. From the simulation result in Fig. 7a), it can be noticed that the most deformations and stresses are evenly located in the second half of the finger, which could effectively prevent the mechanical fatigue. The bent prototype in Fig. 7b) has also verified the deformed shape.

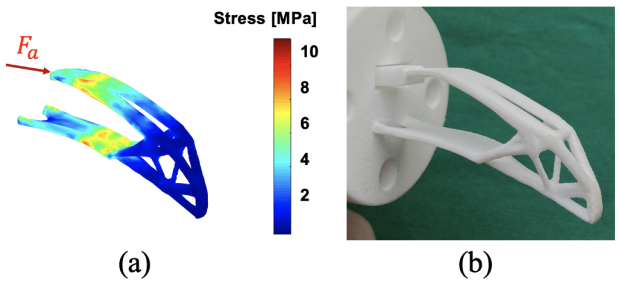

Fig. 7. The bent finger with a displacement-based actuation force F_a of $5\,\mathrm{mm}$: a) The FE-simulated stress distribution, b) The bent prototype.

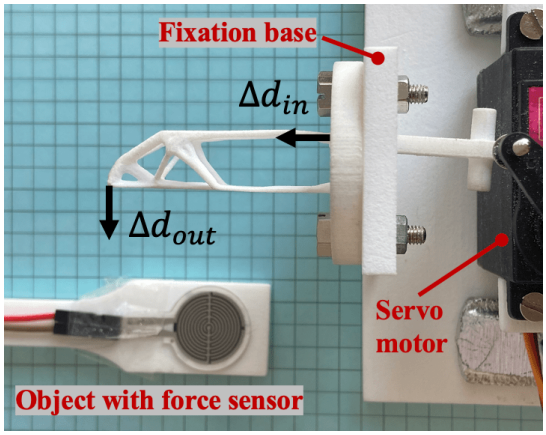

Fig. 8. The experimental setup of the payload test. The force sensor (Film Sensor Technology, China) attached on the object was used to keep the touching force F_t constant.

C. Payload Test

A payload test was also carried out to evaluate the robustness of the realized finger when touching an object. The experimental setup is shown in Fig. 8, where the printed compliant finger was mounted on a platform and actuated by a servo motor to realize the bending movement. In the payload test, a sensor-controlled constant touching force F_t was applied at the tip of the finger while the finger was bent by the actuation force. F_t was chosen as 2 N to imitate the normal touching force of the human finger. The vertical displacement Δd_{out} of the fingertip and the displacement Δd_{in} of the actuation point were measured to analyze the touching force's influence on the bending performance. For comparison, Δd_{in} and Δd_{out} were also measured when no touching force was applied.

The experiment results are reported in Fig. 9. It can be seen that, Δd_{out} increases almost linearly with Δd_{in}. For the untouched (blue curve) and touched (red curve) cases, the largest difference in Δd_{out} is about 2.8 mm, which occurs when $\Delta d_{in} = 0mm$. This small difference in Δd_{out} shows that the realized compliant finger is stable and robust against the normal touching force.

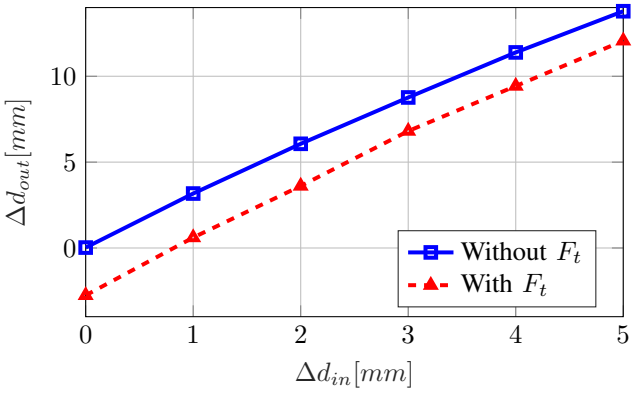

Fig. 9. Trend of the measured fingertip displacements Δd_{out} over the input displacements Δd_{in} (with and without F_t).

IV. Conclusion and Future Work

In this paper, we introduced a 3D topology optimization based framework for designing bionic compliant prosthetic fingers. This work is an extension of our previous work of 2D topology optimization based synthesis [13]–[15]. To evaluate the framework's feasibility, an FE-simulation and a payload test were conducted, which successfully verified the bending performance of the realized compliant finger. In future work, we will use the presented framework to synthesize compliant fingers of different sizes and then, incorporate them into a prosthetic hand to realize sophisticated grasping movements.

References

[1] I. Imbinto, C. Peccia, M. Controzzi, A. G. Cutti, A. Davalli, R. Sacchetti, and C. Cipriani, "Treatment of the partial hand amputation: An engineering perspective," *IEEE Reviews in Biomedical Engineering*, vol. 9, pp. 32–48, 2016.

[2] C. Borst, M. Fischer, S. Haidacher, H. Liu, and G. Hirzinger, "Dlr hand ii: experiments and experience with an anthropomorphic hand," in *2003 IEEE International Conference on Robotics and Automation (Cat. No.03CH37422)*, vol. 1, pp. 702–707 vol.1, 2003.

[3] G. Smit, D. H. Plettenburg, and F. C. T. van der Helm, "The lightweight delft cylinder hand: First multi-articulating hand that meets the basic user requirements," *IEEE Transactions on Neural Systems and Rehabilitation Engineering*, vol. 23, no. 3, pp. 431–440, 2015.

[4] M. Yoshikawa, R. Sato, T. Higashihara, T. Ogasawara, and N. Kawashima, "Rehand: Realistic electric prosthetic hand created with a 3d printer," in *2015 37th Annual International Conference of the IEEE Engineering in Medicine and Biology Society (EMBC)*, pp. 2470–2473, 2015.

[5] L. Liow, A. B. Clark, and N. Rojas, "Olympic: A modular, tendon-driven prosthetic hand with novel finger and wrist coupling mechanisms," *IEEE Robotics and Automation Letters*, vol. 5, no. 2, 2020.

[6] Y. Sun, D. Zhang, Y. Liu, and T. C. Lueth, "Fem-based mechanics modeling of bio-inspired compliant mechanisms for medical applications," *IEEE Transactions on Medical Robotics and Bionics*, vol. 2, no. 3, pp. 364–373, 2020.

[7] H. Zhou, A. Mohammadi, D. Oetomo, and G. Alici, "A novel monolithic soft robotic thumb for an anthropomorphic prosthetic hand," *IEEE Robotics and Automation Letters*, vol. 4, no. 2, pp. 602–609, 2019.

[8] Y. Yan, Y. Wang, X. Chen, C. Shi, J. Yu, and C. Cheng, "A tendon-driven prosthetic hand using continuum structure*," in *2020 42nd Annual International Conference of the IEEE Engineering in Medicine and Biology Society (EMBC)*, pp. 4951–4954, 2020.

[9] Yang Zheng, L. Cao, Zhiqin Qian, Ang Chen, and W. Zhang, "Topology optimization of a fully compliant prosthetic finger: Design and testing," in *2016 6th IEEE International Conference on Biomedical Robotics and Biomechatronics (BioRob)*, pp. 1029–1034, 2016.

[10] H. Zhang, A. S. Kumar, F. Chen, J. Y. H. Fuh, and M. Y. Wang, "Topology optimized multimaterial soft fingers for applications on grippers, rehabilitation, and artificial hands," *IEEE/ASME Transactions on Mechatronics*, vol. 24, no. 1, pp. 120–131, 2019.

[11] Y. Sun and T. C. Lueth, "Sgcl: A b-rep-based geometry modeling language in matlab for designing 3d-printable medical robots," in *2021 IEEE International Conference on Automation Science and Engineering (CASE)*, 2021.

[12] W. E. Lorensen and H. E. Cline, "Marching cubes: A high resolution 3d surface construction algorithm," *ACM siggraph computer graphics*, vol. 21, no. 4, pp. 163–169, 1987.

[13] Y. Sun, Y. Liu, L. Xu, Y. Zou, A. Faragasso, and T. C. Lueth, "Automatic design of compliant surgical forceps with adaptive grasping functions," *IEEE Robotics and Automation Letters*, vol. 5, no. 2, pp. 1095–1102, 2020.

[14] Y. Sun, Y. Liu, L. Xu, and T. C. Lueth, "Design of a disposable compliant medical forceps using topology optimization techniques," in *2019 IEEE International Conference on Robotics and Biomimetics (ROBIO)*, pp. 924–929, IEEE, 2019.

[15] Y. Sun, L. Xu, D. Zhang, and T. C. Lueth, "Automatic synthesis of compliant forceps for robot-assisted minimally invasive surgery," *at - Automatisierungstechnik*, vol. 68, no. 11, pp. 922–932, 2020.